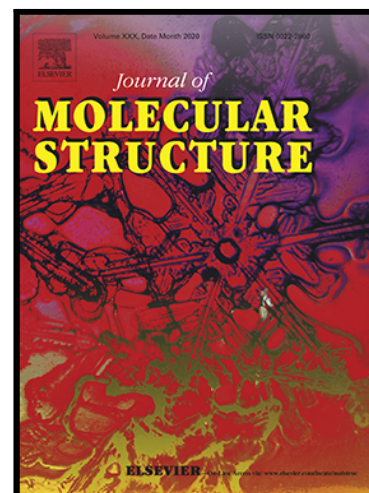


Copper-catalyzed one-pot relay synthesis of anthraquinone based pyrimidine derivative as a probe for antioxidant and antidiabetic activity

Gul Zarren , Nusrat Shafiq , Uzma Arshad , Naila Rafiq ,
Shagufta Parveen , Zaheer Ahmad

PII: S0022-2860(20)31981-5
DOI: <https://doi.org/10.1016/j.molstruc.2020.129668>
Reference: MOLSTR 129668



To appear in: *Journal of Molecular Structure*

Received date: 15 August 2020
Revised date: 1 November 2020
Accepted date: 13 November 2020

Please cite this article as: Gul Zarren , Nusrat Shafiq , Uzma Arshad , Naila Rafiq , Shagufta Parveen , Zaheer Ahmad , Copper-catalyzed one-pot relay synthesis of anthraquinone based pyrimidine derivative as a probe for antioxidant and antidiabetic activity, *Journal of Molecular Structure* (2020), doi: <https://doi.org/10.1016/j.molstruc.2020.129668>

This is a PDF file of an article that has undergone enhancements after acceptance, such as the addition of a cover page and metadata, and formatting for readability, but it is not yet the definitive version of record. This version will undergo additional copyediting, typesetting and review before it is published in its final form, but we are providing this version to give early visibility of the article. Please note that, during the production process, errors may be discovered which could affect the content, and all legal disclaimers that apply to the journal pertain.

Highlights

- One-pot relay synthesis of anthraquinone based-pyrimidine derivatives.
- Novel synergistically active copper catalysts were used in the synthesis.
- Study covers the biological aspects, Molecular docking and QSAR analysis.
- Biologically and theoretically G₂ and G₄ is proposed as an effective compound.
- All the comparative analysis of the advanced techniques are in good agreement.

Copper-catalyzed one-pot relay synthesis of anthraquinone based pyrimidine derivative as a probe for antioxidant and antidiabetic activity

Gul Zarren¹, Nusrat Shafiq^{1*}, Uzma Arshad¹, Naila Rafiq², Shagufta Parveen¹, Zaheer Ahmad³

¹Department of chemistry, Government College Women University Faisalabad-38000

²Department of chemistry, Government College Women University Faisalabad-38000

³Department of chemistry, University of Wah, Wah Cantt.

Corresponding Author: Dr. Nusrat Shafiq, Assistant Professor, Department of chemistry, Government College Women University Faisalabad-38000

Corresponding Address: gqumarin@gmail.com, dr.nusratshafiq@gcwuf.edu.pk

Abstract

Synthetic compounds have modernized the globe due to its vast applicable fields. Anthraquinones, as well as pyrimidine derivatives, are used as essential pharmacophores in the field of medicine. Maintenance of a green disease-free environment by using these derivatives is being acknowledged in developed as well as developing countries of the world. Considering the use of active catalysts in the synthesis of anthraquinone based derivatives are the era of concern for researchers due to their distinctive properties. Owing to the remarkable activities of anthraquinone and pyrimidine derivative, we synthesize compounds having both functionalities with the utilization of novel synergistically active copper catalysts. This study explores the application of synthesized compounds using fast, ecofriendly and cost-effective approaches. ^1H and ^{13}C NMR, antioxidant, antidiabetic, molecular docking and QSAR studies were used for characterization and evaluation of newly synthesized anthraquinone based pyrimidine derivatives. The result of these techniques shows that our desired compounds were successfully synthesized and have potent applications. Among all synthesized compounds, **G₂** and **G₃** showed a remarkable antioxidant activity with IC_{50} of 15.09 and 21.88 $\mu\text{g/ml}$ respectively. While the compound **G₂** and **G₄** showed a strong inhibitory antidiabetic activity with the IC_{50} value of 24.23 and 28.94 $\mu\text{g/ml}$ respectively. Furthermore, molecular docking results for both of the proteins assist the experimental data and confirms the different interactions between binding domains and substituent moieties. SAR study also relates to the experimental facts by giving us positive results of synthesized compounds. According to the QSAR study, **G₄** and **G₂** emerged as the most stable and most reactive compound among other compounds respectively. While MEP shows moderate to good nucleophilic and electrophilic reactivity of all four compounds.

Keywords: Co-crystal approach; Copper catalysis; Antioxidant; Molecular docking; QSAR analysis

Highlights

- One-pot relay synthesis of anthraquinone based-pyrimidine derivatives.
- Novel synergistically active copper catalysts were used in the synthesis.
- Study covers the biological aspects, Molecular docking and QSAR analysis.
- Biologically and theoretically **G₂** and **G₄** is proposed as an effective compound.
- All the comparative analysis of the advanced techniques are in good agreement.

1 Introduction

One of the key sources of potent agents for hundreds of years is the natural and synthetic products. Presently, extraction and application of the natural products as bioactive secondary metabolites in the discoveries of drugs and medicines are the cornerstone of the research field [1]. Various plants produce potent secondary metabolites i.e. anthraquinone, alkaloids and its derivatives which is further used for a wide range of applications in the textile industry, coloring agents and therapeutic agents for the treatment of various diseases [2, 3]. Among secondary metabolites, anthraquinones are found naturally in plants, lichens and fungi. They are widely studied for their structural evaluation and biological significance [4-6]. They are used as laxatives and to treat ulcers, skin disease, tumors, asthma, cancers, itching and eczema [7, 8]. They are also used as antifungal, antimicrobial, insecticidal, antioxidant and as antidiabetic [9-12]. Synthetically, the synthesis of anthraquinone derivative has become the major concern to the chemist to accomplish different chemical strategies. Therefore, various synthetic approaches and their pharmaceutical applications have been examined. In literature, several methods are available for the synthesis of simple to substituted anthraquinone through oxidation of anthracene [13], diels alder reaction [14], and friedel craft reaction [15, 16].

Anthraquinones either synthesized or collected from natural sources are thought to interact with different derivatives having -N group. The anthraquinone due to its planar ring structure permits interaction and intercalation between 5'-pyrimidinepurine-3'GC sites of DNA base pairs in β conformation [17]. Here is the review of some synthetic strategies which were opted in past to synthesize anthraquinone derivatives having -N functionality. The anthraquinone derivatives named ametantrone were synthesized and the final product of the synthesis having two different esterified amino acids L-serine and 6-amino hexanoic acid effectively inhibits the proliferation of cancer cells by intercalating the DNA [18].

Also, anthraquinone based 2-aminopyridine and other anthraquinone derivatives which were coupled with other rings by interaction through -N functionality have been synthesized that shows inactivity against bacteria [19]. The series of dyes having anthraquinone basic nucleus interacted with other groups through N-functionality have been studied that proved to be efficiently used in the medical application for manufacturing the iris implants [20]. Recently, various anthraquinone derivatives with simple to high molecular weight pyrrole and pyrazole rings were synthesized and investigated [3, 21, 22]. All of the above mentioned anthraquinone derivatives interacted directly through the-N functionality either in a ring system or in the aliphatic chain.

After reviewing the literature, we get the point that anthraquinone has a remarkable ability to effectively interact with units having -N functionality. Pyrimidine also consists of a six-membered ring possessing two nitrogen atoms at position 1 and 3 [23]. In addition to many pharmacophores with a variety of potential biological activities, the structural skeleton of pyrimidine is a fundamental constituent of nucleic bases and alkaloids [24]. Like anthraquinone, pyrimidine nucleus present in many classes of chemotherapeutic agents and is in clinical use as an anticancer, antiviral, antifungal, antimalarial and antibacterial agent [25]. Pyrimidine derivatives are cell cycle specific and eradicate only vigorously growing cells [26]. They work by impeding the synthesis of nucleic acid (DNA and RNA) [27].

In recent times, even though there has been a great development in the identification and treatment of diseases, still the treatment of infectious diseases attributes a challenging problem. So, there is a dare need to develop novel and efficient chemotherapeutic agents for treating and controlling outspreading diseases

[28]. As we discussed, heterocyclic compounds having nitrogen moiety exhibit interesting biological activities. The brief overview of remarked chemotherapeutic properties of anthraquinone, pyrimidine and its characteristic interaction with –N based pyrimidine compounds gives us an idea to synthesize compound having both functionalities.

In this study, we intend to synthesize novel anthraquinone based pyrimidine derivatives, which is not discovered yet, through the simple, facile and efficient strategies. Most of the synthetic routes in the past include multiple-step reactions and require expensive catalysts. Therefore, in this study, we follow the facile one-pot protocol as an ideal strategy which not only avoids the formation of multiple bonds, reduce waste production and save time but also give the desired compound having reasonable complexity. Specifically, the coupling reactions catalyzed through the transition metals significantly construct C-C and C-X (X= heteroatom) bond [29]. Hence, we supposed to synthesize our anthraquinone based pyrimidine derivatives catalyzed through these transition metals. Based on this concept, we have used a non-toxic copper catalyst to establish the direct coupling reaction between anthraquinone and pyrimidine derivatives.

2. Materials and Methods

2.1 Chemicals

All the chemicals used in this study were of analytical grade, purchased from a commercial supplier and used without further purification. The following chemicals are used in the synthesis of our first anthraquinone precursor: Phthalic anhydride, Aniline, Phenol, 4-chloro benzaldehyde, Alum and conc. Hydro chloric acid (HCl). Benzaldehyde, 4-chloro-benzaldehyde, urea, ethylacetoacetate and cupric chloride are used in the synthesis of our second pyrimidine precursor. Then Cupric oxide (CuO), Copper chloride (CuCl₂ · 2H₂O), Methanol, Distilled water and both precursors are used in the synthesis of our targeted co-crystal. All the reactions were monitored by TLC and further checked under ultraviolet (254 nm) light.

2.2 General synthesis of precursors

The co-crystal of our desired product was synthesized by the following two steps. The first step is to synthesize anthraquinone derivatives by following the procedure found in the literature with little modification in the synthetic protocol of Madje et al. [15]. A combination of substituted benzene (2g), phthalic anhydride (1g), water (5ml) and a catalytic amount of alum was collectively added in a 50ml one neck round bottom flask. The reaction mixture was allowed to stir for 60-80 minutes at room temperature. The reaction progress was monitored regularly by TLC. After that, the mixture was left until it turns completely in a dry powder form. Then in the product, 3-5ml concentrated HCl was added, the liquid frequently turns yellow. The filtrate was separated and dried to give the solid mass. The crude product was washed with ethyl acetate, dried and checked for its solubility. The synthesized compound was solubilized in methanol, filtered off and recrystallized. The progress of the reaction was again determined with TLC. The schematic representation of the reaction is shown in Fig. . After the successful formation of anthraquinone precursor, we synthesize pyrimidine derivative by following the procedure of Shafiq et al. [30] replacing thiourea with urea. The schematic representation of the reaction is shown in Fig. .

2.3 General synthesis of targeted co-crystal (G₁-G₄)

Anthraquinone derivative (0.2g), pyrimidine derivative (0.2g), methanol (10ml), a catalytic amount of copper chloride and cupric oxide was collectively added in a 100ml one neck round bottom flask. The reaction mixture was allowed to stir for 20-30 minutes at ambient temperature. The reaction progress was monitored regularly by TLC. After the completion of the reaction, the mixture was left till it turns completely in a dry powder form. The formulated compound (Fig. , G₁-G₄) was washed with cold water and dried. The newly synthesized compound was solubilized in hot methanol, filtered off and slowly recrystallized to afford the pure compound. The general schematic representation of reactions is shown in Fig. .

2.4 Characterization

Synthesized compounds obtained in solid form by following the above-mentioned methods were characterized by proton and carbon NMR to validate the successful synthesis of compounds.

2.4.1 N-(9,10-dioxo-9,10-dihydroanthracen-1-yl)-6-methyl-2-oxo-4-phenyl-1,2,3,4-tetrahydropyrimidine-5-carboxamide (G₁, C₂₆H₁₉N₃O₄):

Dark brown solid, % yield: 55, ¹H NMR (300 MHz, DMSO): δ (ppm): 9.14 (s, 1H, NH), 7.69 (m, 2H), 7.69 (m, 2H), 7.57 (m, 2H), 7.52 (m, 1H), 7.27 (m, 2H), 7.20 (m, 2H), 5.09 (d, *J* = 9.5, 0.8 Hz, 2H, NH), 2.50 (d, *J* = 1.0 Hz, 3H, CH₃). ¹³C-NMR (300 MHz, DMSO): δ (ppm): 182.35 (C=O), 180.83 (C=O), 165.7 (C=O), 148.80 (C=O), 145.27 (2C), 131.15 (2C), 128.90 (2C), 127.78 (3C), 126.69 (5C), 99.67 (C), 54.38 (C), 18.28 (CH₃).

2.4.2 Ethyl 4-(4-(9,10-dioxo-9,10-dihydroanthracen-1-ylamino)phenyl)-6-methyl-2-oxo-1,2,3,4-tetrahydropyrimidine-5-carboxylate (G₂, C₂₈H₂₃N₃O₅):

Dark brown solid, % yield: 62, ¹H NMR (300 MHz, DMSO): δ (ppm): 9.24 (s, 1H, NH), 7.97 (s, 1H), 7.97 – 7.90 (m, 1H), 7.77 (m, 1H), 7.53-7.51 (dd, *J* = 7.4, 4.8, 1.8 Hz, 3H), 7.46 (m, 1H), 7.43-7.40 (m, 1H), 7.37 (d, *J* = 9.7 Hz, 1H), 7.25 – 7.25 (m, 2H), 7.22 (m, 2H), 5.14 – 5.13 (m, 3H), 4.01 (1H, NH), 3.98 (m, 2H, CH₂), 2.24 (d, *J* = 0.9 Hz, 3H, CH₃), 1.11 (t, *J* = 8.0 Hz, 3H, CH₃). ¹³C-NMR (300 MHz, DMSO): δ (ppm): 183.14 (C=O), 182.30 (C=O), 165.69 (C=O), 152.41 (C=O), 149.19 (C), 144.21 (C), 132.26 (6C), 129.35 (3C), 128.88 (4C), 128.66 (2C), 99.29 (C), 59.77 (CH₂), 53.85 (CH), 18.25 (CH₃), 14.51 (CH₃).

2.4.3 Ethyl 4-(4-(9,10-dioxo-9,10-dihydroanthracen-1-yloxy)phenyl)-6-methyl-2-oxo-1,2,3,4-tetrahydropyrimidine-5-carboxylate (G₃, C₂₈H₂₂N₂O₆):

Yellow-brown solid, % yield: 60, ¹H NMR (300 MHz, DMSO): δ (ppm): 10.12 (s, 1H, NH), 9.16 (s, 1H, NH), 8.38 – 8.12 (m, 2H), 7.71 (m, 2H), 7.62 (m, 1H), 7.52 (m, 1H), 7.33 (dd, *J* = 7.5, 1.5 Hz, 1H), 7.27 (d, *J* = 9.7 Hz, 2H), 7.20 (m, 2H), 5.09 (d, *J* = 9.7, 0.9 Hz, 1H), 3.95 – 3.90 (m, 2H, CH₂), 2.50 - 2.20 (d, *J* = 1.0 Hz, 3H, CH₃), 1.06 (t, *J* = 8.0 Hz, 3H, CH₃). ¹³C NMR (300 MHz, DMSO): δ (ppm): 192.85 (C=O), 165.75 (C=O), 148.80 (4C), 140.50 (2C), 131.67 (3C), 131.12 (2C), 128.84 (C), 127.71 (2C), 126.67 (C), 124.76 (4C), 99.66 (C), 59.65 (CH₂), 54.38 (CH), 18.23 (CH₃), 14.39 (CH₃).

2.4.4 Ethyl 1-(4-formyl-9,10-dioxo-9,10-dihydroanthracen-1-yl)-6-methyl-2-oxo-4-phenyl-1,2,3,4-tetrahydropyrimidine-5-carboxylate (G₄, C₂₉H₂₂N₂O₆):

Dark Yellow solid, % yield: 53, ¹H NMR (300 MHz, DMSO): δ (ppm): 9.12 (s, 1H, NH), 7.69 (d, *J* = 6.8, 2.1 Hz, 3H), 7.61 (m, 2H), 7.55 (m, 2H), 7.30 (m, 2H), 7.27 – 7.25 (m, 3H), 5.11 (s, 1H, CH), 4.72 (m, 2H, CH₂), 2.20 (s, 3H, CH₃), 1.06 (t, *J* = 8.0 Hz, 3H, CH₃). ¹³C NMR (300 MHz, DMSO): δ (ppm): 182.79

(C=O), 182.36 (C=O), 165.81 (C=O), 148.76 (C=O), 145.14 (2C), 131.29 (7C), 128.85 (2C), 128.75 (3C), 127.78 (3C), 126.66 (3C), 99.78 (C), 59.72 (CH₂), 54.34 (CH), 18.18 (CH₃), 14.48 (CH₃).

2.5 Biological assay

2.5.1 Antioxidant assay

All the synthesized compounds were assessed for their radical scavenging activity by diphenyl picrylhydrazyl (DPPH) free radical. To perform the antioxidant activity, the stock solution of compounds **G₁-G₄** having a concentration 22mg/ml has been prepared. The solutions were then diluted to 250µg, 200µg, 150µg, 100µg and 50µg concentration. DPPH solution of 4mM was prepared in pure methanol. Ascorbic acid was used as a standard. DPPH with methanol was used as a control. In test-tube 1ml of sample/standard solution with 2ml of DPPH solution was added and kept in dark for 30 minutes. Then absorbance of the mixture was measured by using Hitachi U-2900 spectrophotometer at 517nm and expressed as their percentage inhibition, calculated by using the formula mentioned by Marinova and Batchvarov[31].

$$A = \frac{A_{control} - A_{sample}}{A_{control}} \times 100$$

For comparing results, IC₅₀ values of each compound (**G₁-G₄**) were calculated by plotting the graph and performing non-linear regression analysis on GraphPad Prism 8.0.2.

2.5.2 Antidiabetic assay

Antidiabetic activity of all the compounds (**G₁-G₄**) was screened by following the method reported by Eseyin et al. [32] with little modification described here. The mixture containing 0.5ml of sample compound from each diluted solution (250µg, 200µg, 150µg, 100µg and 50µg) along with 0.5ml buffered solution of the enzyme was incubated at room temperature for 10min. After this 0.5ml of the starch solution was added and again incubated for 10min. Then 1ml of DNSA was added to the mixture and kept in boiling water bath for 5 minutes, cooled down and diluted with 20ml of distilled water. The control sample was prepared without any sample mixture. Acarbose was used as a standard. The absorbance of the mixture was taken at 540nm using Hitachi U-2900 spectrophotometer. The inhibitory percentage was calculated using the same formula used for antioxidant activity. For comparing results, IC₅₀ values of each compound (**G₁-G₄**) were calculated from the plots by performing non-linear regression analysis on GraphPad Prism 8.0.2.

2.6 Molecular Docking study

Basically, molecular docking is performed to screen compounds for their biological activity/ potential on the basis of possible orientations and conformations for binding site of ligand. To screen molecules for their activity, first of all, reference molecules (acarbose used standard for anti-diabetic potential and ascorbic acid as standard for anti-oxidant) of respective protein were docked to standardize the protocol. The molecular mechanism of synthesized compounds **G₁-G₄** was explored by conducting molecular docking study by using Molegro Virtual Docker version. Crystal structures of Proteins used for docking analysis were obtained from RSCB protein data bank online at RCSB, <http://www.rcsb.org> and saved as pdb. PDB ID for anti-diabetic activity is human pancreatic amylase (PDB:1HNY) with resolution of 1.8 Å was used as target receptor site whereas for anti-oxidant activity Drosophila melanogaster carboxypeptidase having PDB ID (3MN8) was used as target crystal structure. All these structures were downloaded as

PDB format (gz) [33-35]. Synthesized compounds **G₁-G₄** were drawn in BIOCHEM draw 2D-structures, moved to 3Dbio-Chemdraw by copy-paste and then saved as Mol2 file. Open the docking software and import the protein molecule as pdb. Prepared template and all compounds **G₁-G₄** were run one by one. Before docking, co-factors and water molecules of each protein were removed. Literature study revealed that MVD Molegro Virtual Docker (MVD 2013 6.0.1, Molegro ApS) showed best results for binding affinity in the form of Mol Dock score in comparison to other docking softwares e.g., autodock, Moe, Glide etc. Binding interaction of receptor protein molecule with top rank pose of ligand was observed via hydrogen bonding interactions [33, 35-37]. All the data related to study as parameters like MolDock score, bond length, residues interacting along with groups of ligand interacting were tabulated in tables 3 and 4. All the results of docking for each compound were summarized and discussed in results and discussion (Fig. 6a, 6b, 7a, 7b, 8).

2.7 Quantitative Structure Activity Relationship (QSAR) studies using DFT

Computational studies of synthesized compounds provide us with optimized molecular structures and predict the robustness of molecular reactivity [35]. Quantum mechanically computed descriptors optimized by density functional theory provide the quantitative structure activity relationship for synthesized organic compounds [38, 39]. DFT/B3LYP has been preferred for QSAR studies, optical and electronic properties of compounds because this method is systematic and provides an efficient balance between chemical precision, biological activity and computational tariff [40-42].

2.7.1 Calculation of Micromolecular Descriptors

All synthesized compounds have been computed with Gaussian 09 program favored by the Gauss View 5.1 interface for an imaginal presentation of optimized structures and graphics 39. The molecule is geometrically optimized by using hybrid type B3LYP functional with 321-G basis set in the configuration of DFT, which provides HOMO-LUMO geometries, energy gap, net charge, dipole moment and other molecular descriptors [38, 39]. Quantum chemical parameters based upon DFT computations for the purpose of SAR studies at DFT/B3LYP/3-21G(d) were calculated.

3 Results and Discussion

A novel sequential synthesis of anthraquinone based pyrimidine derivatives has been done through a one-pot relay process. Firstly, anthraquinone and pyrimidine derivatives have been synthesized according to the methods found in the literature with little modification mentioned above in the synthesis protocol. Then by combining both of the precursors in the presence of a suitable catalyst, our novel targeted co-crystal have been synthesized. To assess the synthetic process for the preparation of anthraquinone based pyrimidine derivatives, we explored the conditions required to simply combine our model substrate that is anthraquinone derivative **3** and pyrimidine derivative **5**. It has already been recognized that among the transition metal catalyst, copper (Cu) catalyst proved to be potently used in several organic syntheses. Copper contributes to effectively catalyze several reactions like C-C and C-N cross-coupling, heterocyclic synthesis, amide linkage formation and conjugate addition [39, 41]. According to one school of thought,

copper catalyst along with some metal oxides synergistically enhance the selective conversion. Copper together with metal oxide provide a basic metal site to simultaneously accelerate the retro aldol condensations and isomerization reaction [43]. Recently, studies have shown that copper oxide synergistically coactive copper chloride and facilitate the electrophilic reactions [44]. Therefore, after exploring the conditions required for the subsequent reaction, copper chloride along with cupric oxide as a catalyst and methanol as a solvent was used to make our coupling reaction feasible. The overall one-pot relay procedure involves intermolecular coupling reaction between anthraquinone **3** and pyrimidine **5** derivatives catalyzed through synergistically active copper catalyst to form four novel anthraquinone based pyrimidine derivatives (**G₁-G₄**) as shown in Fig. . After the successful synthesis, all the synthesized compounds were confirmed through the interpretation of their spectral data.

The ¹H-NMR and ¹³C-NMR spectra of compound **G₁-G₄** showed characteristic peaks which enable us to identify and characterize the corresponding compounds. The ¹H-NMR spectra of **G₁** displayed characteristic protonic singlet peak at δ 9.14 which confirms the presence of amide group present at the junction of the anthraquinone and pyrimidine ring. While the characteristic carbon peak in the ¹³C-NMR of **G₁** at δ 165.7 is due to carbonyl functionality directly linked with –NH group. These distinguishing peaks of **G₁** confirm the successful formation of our targeted product.

All other peaks of anthraquinone and pyrimidine rings in the spectra of compound **G₁** are in consonance with the literature [45].

The ¹H-NMR spectra of **G₂** showed a characteristic protonic singlet peak at δ 4.01 is due to –NH group which joins the anthraquinone and pyrimidine ring together. While the little upfield chemical shift value at 144.21 and 132.26 ppm in the ¹³C-NMR of **G₂** is due to the effect of directly linked –NH group. These distinguishing peaks of **G₂** confirm the successful linkage between anthraquinone and pyrimidine ring. All other peaks of anthraquinone and pyrimidine rings in the spectra of compound **G₂** are similar to **G₁** except the additional peaks at δ 3.98 and 1.11 in ¹H-NMR and 59.7 and 14.5 in ¹³C-NMR which originates due to the presence of –OC₂H₅ group. In the ¹H-NMR spectra of **G₃** the missing singlet peak at δ 5.00, which should be shown in case of the presence of unreacted hydroxyanthraquinone, confirms that there must be a linkage. While in the ¹³C-NMR spectra of the same compound, the characteristic upfield chemical shift values of carbon at 148.80 ppm shows that these carbons must be attached directly in C-O-C linkage. These two characteristic peaks confirm the successful synthesis of our compound **G₃**. All other peaks of anthraquinone and pyrimidine rings in the spectra of compound **G₃** are similar to **G₂**.

In the ¹H-NMR spectra of **G₄** again one missing singlet peak of –NH at δ 9.00-10.00, which should there if pyrimidine derivative left unreacted, confirms that there must be some sort of linkage. While the ¹³C-NMR spectra of the same compound showed the distinctive up field chemical shift value of carbon at 148.80 ppm. This distinguishing peak shows that this carbon must be directly attached to the –NR group.

Here both the characteristic peak values confirm the successful formation of compound **G₄**. Furthermore, all other peaks of anthraquinone and pyrimidine rings in the spectra of compound **G₄** are similar to **G₂** except the additional protonic peak at δ 9.12 which arises due to the presence of the aldehyde group.

3.1 Biological evaluation

3.1.1 Antioxidant activity

Unstable free radicals have shown a main role in developing a number of diseases and antioxidants are primarily the source of eliminating these radicals by inhibiting the oxidation rate and protecting the body from damage [46]. Oxidative stress caused by these free radicals in atherosclerosis, stroke, diabetes and a number of other diseases are treated with antioxidants nowadays [47, 48]. In order to evaluate in vivo and in vitro antioxidant activity, several procedures have been developed recently [49-51]. In our study, the antioxidant ability of our compound was evaluated by DPPH radical scavenging activity. DPPH is known to be one of the stable free radical that can accept an electron or hydrogen radical from the corresponding donor to form a diamagnetic molecule. When the DPPH accepts a hydrogen from donor, its solution readily convert from dark purple to yellow [52-54]. In vitro antioxidant activity of all the synthesized compounds (**G₁-G₄**) have shown the results summarized in Table 1. Standard ascorbic acid show 51.25 percent inhibition. At various concentration, compound **G₁-G₄** were screened for their percent inhibition. In comparison to standard ascorbic acid, compound **G₃** with a concentration of 50 μ g/ml have shown the excellent antioxidant activity with 49.75 percent inhibition. While the other compounds **G₁**, **G₂** and **G₄** have shown the maximum 30.78, 45.76 and 36.94 percent inhibition respectively with moderate to good antioxidant activity as compared to the standard ascorbic acid.

To compare the overall results, we have calculated the IC₅₀ value for each sample compound through GraphPad Prism analysis and the results are shown in Fig. . The lower IC₅₀ values indicate the greater antioxidant activity of compounds. Certainly, the compound **G₂** and **G₃** showed the excellent DPPH radical scavenging activity with IC₅₀ of 15.09 and 21.88 μ g/ml respectively. This remarked activity may be attributed to the combined effect of anthraquinone and pyrimidine precursor. While the other two compounds i.e. **G₁** and **G₄** have shown a weak inhibitory activity with the IC₅₀ value of 64.31 and 97.51 μ g/ml respectively due to the structural differences of compounds.

3.1.2 Antidiabetic activity

The disease of high blood glucose levels is characterized as diabetes, which becomes a serious problem nowadays. So, the main goal of the scientist is to develop treatment or medication that can effectively treat diabetes by controlling the levels of blood sugar. In this modern age, there is a great development in the field of medication or treatment which can treat diabetes with hyperglycemia and hypoglycemia agents [55, 56]. Despite these developments, all the treatment modes and medications are still related to some side effects which opens up the ways for further investigation. In this study, we have checked the antidiabetic activity of newly synthesized compounds (**G₁-G₄**) by in vitro alpha-amylase analysis. In vitro antidiabetic activity of all the synthesized compounds have shown the results summarized in Table 2. Acarbose was used as a standard and exhibit 61.70 percent inhibition. At various concentration, compound **G₁-G₄** were screened for their percent inhibition. In comparison to standard acarbose, compound **G₂** exhibits good antidiabetic activity with 57.80 percent inhibition. While the other

compounds **G₁**, **G₄** and **G₃** in comparison to standard acarbose have shown moderate antidiabetic activity with a maximum 40.96, 39.36 and 37.94 percent inhibition respectively. Furthermore, the inhibitory effects of each synthesized compound were evaluated with the calculation of IC₅₀ which interprets the concentration of the inhibitor that is required to inhibit 50% of its targeted enzyme. The lower IC₅₀ values indicate the greater antidiabetic activity of compounds. In comparison to the overall result, compound **G₂** and **G₄** (Fig.) showed a strong inhibitory activity with an IC₅₀ value of 24.23 and 28.94 µg/ml. respectively. Whereas, the other compounds i.e. **G₁** and **G₃** have shown a weak inhibitory activity with the IC₅₀ value of 89.37 and 78.82 µg/ml respectively. The overall difference showed in the results may be attributed to the structural differences of a compound.

3.2 Molecular Docking study analysis

Docking studies were performed to explore the action mechanism of targeted compounds **G₁-G₄** as antidiabetic and antioxidant agents. **G₁-G₄** showed multiple interactions with active sites of binding proteins receptors (**Error! Reference source not found.**a, 6b, 7a, 7b and 8) explored by Docking results. The more feasible binding modes of molecules **G₁-G₄** for anti-diabetic protein (human pancreatic alpha amylase) revealed their docking score range from -119.48 to -131.536 Kcal/mol while of standard drug acarbose used was -111.57 kcal/mol respectively. Best possess of ligand that fit into receptor sites were observed in MVD. **G₁** and **G₃** compounds showed zero interactions (Fig. 6a-b and table 3). **G₂** showed two interactions as oxygen of 30-O with Thr 163 and oxygen of aldehyde group at 11' with His 305 having bond lengths of 2.602 and 2.44 Å° respectively (Fig. 6a-b). Compound **G₄** interact with Ile 235 by its oxygen of aldehyde group at 11'-position having bond length of 2.89 Å° (Fig. 6a-b and Table 3). Capacity of all compounds **G₁-G₄** for binding affinity and anti-diabetic activity were observed in a good correlation. Experimental results of antidiabetic activity of compound **G₂** showed best %age inhibition among all compounds (Tale 2) which was in accordance with MolDock scores and additionally quantity of hydrogen bond interactions with receptor also confirm the **G₂** as a good inhibitor of target enzyme [56, 57].

Synthesized compounds were further screened for their antioxidant potential by using ascorbic acid as standard. Their molecular docking results showed that best fit modes of compounds **G₁-G₄** have Mol dock score in range of -131.96 to -184.273 kcal/mol while standard ascorbic acid has mol dock score of -80.346 kcal/ mol (Table 4). From molDock score it has cleared that all the compounds **G₁-G₄** have good anti-oxidant activity as compared to standard (Fig. 7a-b, Tble 4)[55]. 3D interface of best fit poses as ligand into receptor site are shown in MVD. In vitro anti-oxidant activity of synthesized compounds is greatly correlated with molecular docking results. Compound **G₁** showed three interactions with receptor as 15-O with Lys 370, 16-O with Gln 79 and 31-O with Ser 86 having bond lengths of 2.72, 2.61 and 3.27 Å° respectively. **G₂** showed only two interactions of 15-O with Lys 208 and oxygen of aldehyde at 11-position with Arg 367 having bond lengths of 3.091 and 3.093 Å° respectively whereas compound **G₄** also have three hydrogen bond interactions as; oxygen of aldehyde group at 11'-position with Lys 370 at distance of 3.108 Å, 15-O and 28-O with Asn 203 at bond length of 3.17 and 3.01 Å respectively (Fig. 7a-b and table 4). Among all compounds, **G₃** showed interactions as 15-O linked with Rag 68 and 16-O linked with Asn 203 having hydrogen bond lengths of 3.58 and 3.41 Å° respectively. 25-NH and oxygen of aldehyde present at 26-position interact with same receptor Phe 65 at different bond lengths 2.60 and

3.1 Å. Likewise, 30-O and 31-O interact with Ser 207 at distance of 3.10 and 2.60 Å respectively [33, 56, 58]. In case of ascorbic acid, it's all hydroxyl group that showed hydrogen bonding interactions with Lys 370, Ser 207, Arg 87, Ser 369 and oxygen of ring showed interaction with Lys 370 respectively. Length of all the hydrogen bonds involved were found within the range 2.83 -3.28 Å (Fig.8, Table 4) [57, 59].

By observing tabulated data (

Table 3 and

Table 4), it has been confirmed that the differences of interactions were due to structural differences among target molecule **G₁-G₄** and this theoretical data was found very close to experimental data evaluated for their biological action mechanism. Docking results (

Table 3) explored the maximum interactions for **G₂** in PDB:1NHY and pose which reflect maximum interaction was shown in **Error! Reference source not found.a-b**. Docking results for PDB:3MN8 (

Table 4) were displayed that the maximum interactions were found for **G₃** (**Error! Reference source not found.**a-b) and this confirmed the **G₃** as an excellent inhibitory agent. By comparing these results, it was suggested that inhibitory potential of compounds **G₁-G₄** is due to their interactions with their binding domains and dependent upon substituent moieties.

3.3 Quantitative Structure Activity Relationship (QSAR) analysis

Quantitative Structure Activity Relationship analysis of our compounds (**G₁-G₄**) leads us to fundamental results which are discussed below.

3.3.1 Global Reactivity Descriptors

Electronegativity (χ), chemical potential (μ), global hardness (η), global softness (S), electrophilicity index (ω) and Electronic energy (E) are the molecular reactivity parameters.

Table 5 showed the calculated values for each synthesized compound. Dipole moment (μ) is the measure of the bond properties and charge densities in the molecule. Fig. showed the vector of the dipole moment of all the synthesized compounds. Compound **G₃** has a large value of dipole moment which showed that it has the best charge distribution and increasing distance of bonds. This means that compound **G₃** showed the best conductivity improved through oxidation [60]. Highest electrophilicity value ($\omega = 0.086$ eV) and electronegativity values ($\chi = 0.1720$ eV) indicate that compound **G₄** is the best electron acceptor or good electrophile [61]. The large negative value of electronic energy (E) indicates the stability of compound **G₄** as compared to other compounds that referred to the Coulombic forces, dipole-dipole interactions and hydrogen bonds contributed towards the higher binding affinity, more solute-solvent interactions and low IC_{50} value [62]. Hence, the low antidiabetic IC_{50} value of compound **G₄** (Table 2) is proved to be in accordance with this theoretical evaluation.

3.3.2 Molecular Electrostatic Potential (MEP)

MEP help to predict the hydrogen bonding interaction, molecular recognition process and interpretation of electrophilic and nucleophilic reactions. This model is the check of responsiveness of molecule towards a binding substrate and behavior of molecule with other compounds. Also, this modal is a visual scheme for checking the relative polarity of the molecule. Fig. showed the molecular electrostatic potential map based on SCF energy. The positive (blue) region of molecular electrostatic potential showed nucleophilic reactivity while the negative (red and yellow) regions showed the electrophilic reactivity [36]. The blue color is an indication of the site of the nucleophilic attack, in all the compounds, hydrogen atoms are capable to react with a nucleophile. While red or yellow color is an indication of an electrophilic attack, so all the oxygen atoms are capable to react with an electrophile. While benzene rings remain neutral as green color indicates the neutral reactivity [63].

3.3.3 Frontier Molecular Orbital Analysis (FMO)

According to this theory, HOMO and LUMO are vital factors as these orbitals are modeled for molecular reactivity and pharmacological properties. In which HOMO acts as an electron donor and LUMO acts as an electron acceptor. Fig. shows the energy level and dispersion of LUMO and HOMO orbitals calculated at the B3LYP/3-21G(d) [64].

Values of HOMO and LUMO predicted that HOMO is more stable than the LUMO and energy gap having small difference showed that molecule is soft, tend to be more polarized and biologically active in inhibiting the enzymatic activity. This energy gap showed that the molecule is chemically more reactive and kinetically less stable [63]. Homo is related to ionization potential and LUMO is linked to electron affinity [40, 44].

Compound **G₁** has the highest value of HOMO energy ($E_{HOMO} = -0.06878$ eV). In the same way, the compound **G₄** has the lowest value of LUMO energy ($E_{LUMO} = -0.11641$ eV). HOMO-LUMO diagram of four compounds (Fig.) showed that the best electron donor moieties in the molecules are amide group and the oxygen atoms of the quinoline molecule. In the same way, the best electron moiety is the anthraquinone moiety of the **G₄** compound due to the presence of LUMO orbitals on this moiety. The compound **G₂** has the lowest energy gap ($\Delta E_{gap} = 0.10122$ eV) which tends to make it softer and more

reactive as compared to another molecule. Chemical hardness and softness of **G₂** ($\eta = 0.05061$ eV, $S = 9.8794$ eV) are lesser among all molecules so the molecule is more reactive of all other compounds [61].

Conclusively, the compounds are optimized by using density functional theory calculations using B3LYP as a basis set with 3-21G as a functional level using Gaussian 09 package. FMO studies showed that compound **G₂** has a lower energy gap, therefore, considered to be more reactive as compared to all other compounds. Hence, compound **G₂** showed the best antioxidant and antidiabetic activities described in biological evaluation, which is in accordance with its theoretical results. Molecular electrostatic potential studies showed that all the compounds have positive region around hydrogen atoms and the negative region around the oxygen atom of carbonyl groups and anthraquinone group [33]. Other reactivity parameters calculations shown in

Table 5 confirm that these electronic properties help us to synthesize the leading compound for future research.

4 Conclusion

The summary of our whole work is as follows. Four new biologically active compounds **G₁**, **G₂**, **G₃** and **G₄** were synthesized in a one-step procedure by the incorporation of substituted anthraquinone and pyrimidine derivatives. The incorporation of these derivatives was done by the one-pot relay process using a synergically active copper catalyst. Among the four novel compounds, the compound ethyl 4-(4-(9,10-dioxo-9,10-dihydroanthracen-1-ylamino) phenyl) -6-methyl-2-oxo-1,2,3,4-tetrahydropyrimidine-5-carboxylate (**G₂**) showed remarkable biological applications and proved to be a potent antioxidant and antidiabetic drug. Other synthesized compounds showed good to moderate biological applications. Molecular docking results further assist the experimental results and confirms that among all the synthesized compounds (**G₁-G₄**), ethyl-4-(4-(9,10-dioxo-9,10-dihydroanthracen-1-yloxy) phenyl)-6-methyl-2-oxo-1,2,3,4-tetrahydropyrimidine-5-carboxylate (**G₃**) showed maximum interactions with both evaluated proteins. QSAR analysis further relates to the experimental study and shows superior stability of compound **G₄** with the large negative value of electronic energy and low IC₅₀ value of this compound. Also, MEP predicts the hydrogen bonding interaction and shows the reactivity of all four compounds having moderate to good nucleophilic and electrophilic reactivity. Furthermore, FMO analysis gives us confidence about the synthesis and successful application of our novel compounds and showed the lower energy gaps and higher reactivity of compound **G₂** compared to all other compounds, which is in accordance with the experimental results of the biological analysis. Hence, overall the compounds synthesized here proved to be the potential compounds that may cause evolutionary success in the field of medicine and synthesis. Conclusively, the synthetic strategy opted here can be of prime interest for the research community and the novel compounds synthesized here can be used in the future as an effective organic drug due to their safety, inexpensive, sustainability, enhanced activity and eco-friendly nature.

Credit Author Statement

Gul Zarren¹: Methodology, Experimental and writing related portion

Nusrat Shafiq^{1*}: Conceptualization, Designing Reactions and research theme, Molecular Docking study, Writing- reviewing

Uzma Arshad¹: DFT calculations, visualization, Software Validation and writing related portion

Naila Rafiq²: Bioactivity Portion writing

Shagufta Parveen¹: Reviewing and Editing

Zaheer Ahmad³: Supervision

Declaration of Competing Interest

The authors declare that they have no known competing financial interests or personal relationships that could have appeared to influence the work reported in this paper.

There is no conflict of interest

Acknowledgement

Authors are thankful to Higher Education Commission of Pakistan to provide facilities to conduct this research under HEC/SRGP.1142 research Grant.

References

- [1] P. Wangchuk, Therapeutic applications of natural products in herbal medicines, biodiscovery programs, and biomedicine, *Journal of Biologically Active Products from Nature* 8(1) (2018) 1-20.
- [2] N. Brihi, Pharmacological activity of alkaloids: a review, *Asian J Botany* 1 (2018) 1-6.
- [3] A.S. Tikhomirov, A.A. Shtil, A.E. Shchekotikhin, Advances in the discovery of anthraquinone-based anticancer agents, *Recent patents on anti-cancer drug discovery* 13(2) (2018) 159-183.
- [4] A.T. Sougiannis, B. Kelley, K.E. Velazquez, R.T. Enos, J.E. Bader, I. Chatzistamou, M.M. Pena, M. Nagarkatti, s.A. Carson, D. Fan, Emodin, a natural anthraquinone, may help protect gastrointestinal health during chemotherapy treatment by decreasing inflammation of the gastric mucosa and preserving gut morphology, *The FASEB Journal* 33(1_supplement) (2019) 368.2-368.2.
- [5] P. Sudhakar, V.V. Prabhu, B. Jamuna, R. Adithya, A. Joy, R. Anand, Preclinical toxicological evaluation of Aloe vera health drinks in wistar rats, *International Journal of Research in Pharmaceutical Sciences and Technology* 1(1) (2018) 27-32.
- [6] Y.-Q. He, Q. Zhang, Y. Shen, T. Han, Q.-L. Zhang, J.-H. Zhang, B. Lin, H.-T. Song, H.-Y. Hsu, L.-P. Qin, Rubiadin-1-methyl ether from *Morinda officinalis* How. Inhibits osteoclastogenesis through blocking RANKL-induced NF- κ B pathway, *Biochemical and biophysical research communications* 506(4) (2018) 927-931.
- [7] G. Srinivas, S. Babykutty, P.P. Sathiadevan, P. Srinivas, Molecular mechanism of emodin action: transition from laxative ingredient to an antitumor agent, *Medicinal research reviews* 27(5) (2007) 591-608.
- [8] M.M. Mohammed, S.S. El-Souda, S.M. El-Hallouty, N. Kobayashi, Antiviral and cytotoxic activities of anthraquinones isolated from *Cassia roxburghii* Linn. leaves, *Herba Polonica* 59(4) (2013) 33-44.
- [9] X.-F. Shang, Z.-M. Zhao, J.-C. Li, G.-Z. Yang, Y.-Q. Liu, L.-X. Dai, Z.-J. Zhang, Z.-G. Yang, X.-L. Miao, C.-J. Yang, Insecticidal and antifungal activities of *Rheum palmatum* L. anthraquinones and structurally related compounds, *Industrial Crops and Products* 137 (2019) 508-520.
- [10] W. Wang, R. Chen, Z. Luo, W. Wang, J. Chen, Antimicrobial activity and molecular docking studies of a novel anthraquinone from a marine-derived fungus *Aspergillus versicolor*, *Natural product research* 32(5) (2018) 558-563.

- [11] A. Mohammed, M.A. Ibrahim, N. Tajuddeen, A.B. Aliyu, M.B. Isah, Antidiabetic potential of anthraquinones: A review, *Phytotherapy Research* (2019).
- [12] D. Petzold, B. König, Photocatalytic Oxidative Bromination of Electron-Rich Arenes and Heteroarenes by Anthraquinone, *Advanced Synthesis & Catalysis* 360(4) (2018) 626-630.
- [13] Y.-G. Wang, X.-Y. Wei, S.-K. Wang, R.-L. Xie, P. Li, F.-J. Liu, Z.-M. Zong, A FeCl₃-based ionic liquid for the oxidation of anthracene to anthraquinone, *Fuel processing technology* 135 (2015) 157-161.
- [14] L. Gogin, E. Zhizhina, Z. Pai, One-Pot Process to Produce Anthraquinone Derivatives: Prospective Wood Delignification Catalysts, *Kinetics and Catalysis* 59(5) (2018) 578-584.
- [15] B.R. Madje, K.F. Shelke, S.B. Sapkal, G.K. Kakade, M.S. Shingare, An efficient one-pot synthesis of anthraquinone derivatives catalyzed by alum in aqueous media, *Green Chemistry Letters and Reviews* 3(4) (2010) 269-273.
- [16] B. Madje, M. Ubale, J. Bharad, M. Shingare, B (HSO₄) 3: an efficient solid acid catalyst for the synthesis of anthraquinone derivatives, *Bulletin of the Catalysis Society of India* 9(2) (2011) 19-25.
- [17] A. Adhikari, K.S. Mahar, DNA targeted anthraquinone derivatives: an important anticancer agents, *International Journal of Pharmacy and Pharmaceutical Sciences* 8 (2016) 17-25.
- [18] H. Sadeghi-Aliabadi, M. Tabarzadi, A. Zarghi, Synthesis and cytotoxic evaluation of two novel anthraquinone derivatives, *Il Farmaco* 59(8) (2004) 645-649.
- [19] N.B. Patel, A.L. Patel, New 2-aminopyridine containing acid anthraquinone dyes, their application and microbial studies, *Indian Journal of Chemistry* 48(B) (2009) 705-711.
- [20] C. Dollendorf, S.K. Kreth, S.W. Choi, H. Ritter, Polymerization of novel methacrylated anthraquinone dyes, *Beilstein journal of organic chemistry* 9(1) (2013) 453-459.
- [21] M. Gouda, M. Berghot, A. Shoeib, A. Khalil, Synthesis and antimicrobial of new anthraquinone derivatives incorporating pyrazole moiety, *European journal of medicinal chemistry* 45(5) (2010) 1843-1848.
- [22] A.S. Tikhomirov, E.E. Bykov, Y.N. Luzikov, A.M. Korolev, A.E. Shchekotikhin, Heterocyclic analogs of 5, 12-naphthacenequinone 13*. Synthesis of 4, 11-diaminoanthra [2, 3-b] furan-5, 10-diones and sulfur-containing analogs, *Chemistry of Heterocyclic Compounds* 52(10) (2016) 797-802.
- [23] A. Verma, L. Sahu, N. Chaudhary, T. Dutta, D. Dewangan, D. Tripathi, A review: Pyrimidine their chemistry and pharmacological potentials, *Asian J. Biochem. Pharm. Res* 2 (2012) 2231-2560.
- [24] W. El-Sayed, I. Zeid, E. Morsi, N. Tawfek, N. Yousif, S. Yahia, A. Abdel-Rahman, Synthesis and Anticancer Activity of New Substituted Pyrimidines, Their Bicyclic and Thioglycoside Derivatives, *Life Science Journal* 12(6) (2015) 63-70.
- [25] S. Sridhar, Y.R. Prasad, S. Dinda, Synthesis and anticancer activity of some novel pyrimidine derivatives, *International Journal of Pharmaceutical Sciences and Research* 2(10) (2011) 2562-2565.
- [26] S.D. Arikatt, M. Chandran, A. Bhat, K. Krishnakumar, Synthesis and molecular docking studies of few novel Pyrimidine derivatives, *Journal of Pharmacy Research Vol* 8(2) (2014) 93-97.
- [27] T. Utsugi, New challenges and inspired answers for anticancer drug discovery and development, *Japanese journal of clinical oncology* 43(10) (2013) 945-953.
- [28] A.M. Mohamed, H.R. Al-Qalawi, W. El-Sayed, W.A. Arafa, M.S. Alhumaimess, A.K. Hassan, Anticancer activity of newly synthesized triazolopyrimidine derivatives and their nucleoside analogs, *Acta Poloniae Pharm. Drug Res* 72 (2015) 307-318.
- [29] B. Suchand, G. Satyanarayana, Palladium-Catalyzed Direct Acylation: One-Pot Relay Synthesis of Anthraquinones, *Synthesis* 51(03) (2019) 769-779.
- [30] N. Shafiq, S. Ashraf, S. Parveen, B. Ali, A One-pot Rapid Synthesis, Docking Study and Biological Evaluation of Some Tetrahydropyrimidine-5-carboxylates, *Indian Journal of Heterocyclic Chemistry* 29(3) (2019) 249-253.
- [31] G. Marinova, V. Batchvarov, Evaluation of the methods for determination of the free radical scavenging activity by DPPH, *Bulgarian Journal of Agricultural Science* 17(1) (2011) 11-24.

- [32] O.A. Eseyin, E. Edem, E. Johnson, A. Ahmad, S. Afzal, Synthesis and in vitro antidiabetic activity of some alkyl carbazole compounds, *Tropical Journal of Pharmaceutical Research* 17(3) (2018) 537-541.
- [33] M.N. Ahmed, K.A. Yasin, S. Hameed, K. Ayub, I.-u. Haq, M.N. Tahir, T. Mahmood, Synthesis, structural studies and biological activities of three new 2-(pentadecylthio)-5-aryl-1, 3, 4-oxadiazoles, *Journal of Molecular Structure* 1129 (2017) 50-59.
- [34] S. Bouchagra, F. Benamia, Z. Djeghaba, Docking studies of (-)-Epigallocatechin-3-gallate: A potential non-competitive pancreatic lipase inhibitor, *Research Journal of Pharmaceutical, Biological and Chemical Sciences* 7(5) (2016) 2493-2505.
- [35] M. Horchani, A. Hajlaoui, A. HalimHarrath, L. Mansour, H.B. Jannet, A. Romdhane, New pyrazolo-triazolo-pyrimidine derivatives as antibacterial agents: Design and synthesis, molecular docking and DFT studies, *Journal of Molecular Structure* 1199 (2020) 127007.
- [36] W. Kohn, A.D. Becke, R.G. Parr, Density functional theory of electronic structure, *J. Phys. Chem.* 100(31) (1996) 12974-12980.
- [37] V.J.J.O.M. Reenu, Exploring the role of quantum chemical descriptors in modeling acute toxicity of diverse chemicals to *Daphnia magna*, *Journal of Molecular Graphics and Modelling* 61 (2015) 89-101.
- [38] D.E. Arthur, A. Uzairu, P. Mamza, S.E. Abechi, G. Shallangwa, Insilico study on the toxicity of anti-cancer compounds tested against MOLT-4 and p388 cell lines using GA-MLR technique, *Beni-Suef University Journal of Basic and Applied Sciences* 5(4) (2016) 320-333.
- [39] A. M.Farag, A. M.Fahim, Synthesis, biological evaluation and DFT calculation of novel pyrazole and pyrimidine derivatives, *Journal of Molecular Structure* 1179 (2019) 304-314.
- [40] A.K. Srivastava, N. Misra, A comparative theoretical study on the biological activity, chemical reactivity, and coordination ability of dichloro-substituted (1,3-thiazol-2-yl)acetamides, *Canadian Journal of Chemistry* 92(3) (2014) 234-239.
- [41] U.O. Ozdemir, F. İlbiz, A.B. Gunduzalp, N. Ozbek, Z.K. Genç, F. Hamurcu, S. Tekin, Alkyl sulfonic acide hydrazides: Synthesis, characterization, computational studies and anticancer, antibacterial, antiepileptic anhydrase II (hCA II) activities, *Journal of Molecular Structure* 1100 (2015) 464-474.
- [42] S.R. Chemler, Copper catalysis in organic synthesis, *Beilstein J. Org. Chem.* 11 (2015) 2252-2253.
- [43] C. Liu, Z. Zhang, X. Zhai, X. Wang, J. Gui, C. Zhang, Y. Zhu, Y. Li, Synergistic effect between copper and different metal oxides in the selective hydrogenolysis of glucose, *New Journal of Chemistry* 43(9) (2019) 3733-3742.
- [44] D. Wang, H. Zhang, Y. Fan, R. Cao, Y. Gao, J. Chen, Synergistic effect of mixed Cu and Fe oxides and chlorides on electrophilic chlorination of dibenzo-p-dioxin and dibenzofuran, *Science of The Total Environment* 721 (2020) 137563.
- [45] K. Huang, L. Jiang, H. Li, D. Ye, L. Zhou, Development of Anthraquinone Analogues as Phosphoglycerate Mutase 1 Inhibitors, *Molecules* 24(5) (2019) 845-864.
- [46] O.A. Asimi, N. Sahu, A. Pal, Antioxidant activity and antimicrobial property of some Indian spices, *International Journal of Scientific and Research Publications* 3(3) (2013) 1-8.
- [47] T. Devasagayam, J. Tilak, K. Boloor, K.S. Sane, S.S. Ghaskadbi, R. Lele, Free radicals and antioxidants in human health: current status and future prospects, *J assoc Physicians India* 52(794804) (2004) 794-804.
- [48] A.B.R. Khalipha, F. Ahmed, M.M. Rahman, Antioxidant and antidiarrhoeal potentiality of *Diospyros blancoi*, *International Journal of Pharmacology* 8(5) (2012) 403-409.
- [49] M.F. Zayed, R.A. Mahfoze, S.M. El-kousy, E.A. Al-Ashkar, In-vitro antioxidant and antimicrobial activities of metal nanoparticles biosynthesized using optimized *Pimpinella anisum* extract, *Colloids and Surfaces A: Physicochemical and Engineering Aspects* 585 (2020) 124167.
- [50] J. Mo, T. Chen, H. Yang, Y. Guo, Q. Li, Y. Qiao, H. Lin, F. Feng, W. Liu, Y. Chen, Design, synthesis, in vitro and in vivo evaluation of benzylpiperidine-linked 1, 3-dimethylbenzimidazolinones as

- cholinesterase inhibitors against Alzheimer's disease, *Journal of Enzyme Inhibition and Medicinal Chemistry* 35(1) (2020) 330-343.
- [51] P.C. Nobre, H.A. Vargas, C.G. Jacoby, P.H. Schneider, A.M. Casaril, L. Savegnago, R.F. Schumacher, E.J. Lenardão, D.S. Ávila, L.B.R. Junior, Synthesis of enantiomerically pure glycerol derivatives containing an organochalcogen unit: in vitro and in vivo antioxidant activity, *Arabian Journal of Chemistry* 13(1) (2020) 883-899.
- [52] K. Prashith, M. Manasa, G. Poornima, V. Abhipsa, C. Rekha, S.P. Upashe, H. Raghavendra, Antibacterial, Cytotoxic and Antioxidant Potential of *Vitex Negundo* Var. *Negundo* and *Vitex Negundo* Var. *Purpurascens*—A Comparative Study, *Science, Technology and Arts Research Journal* 2(3) (2013) 59-68.
- [53] G. Tirzitis, G. Bartosz, Determination of antiradical and antioxidant activity: basic principles and new insights, *Acta Biochimica Polonica* 57(2) (2010) 139-142.
- [54] Q.U. Ahmed, B.B. Dogarai, M. Amiroudine, M. Taher, J. Latip, A. Umar, B.Y. Muhammad, Antidiabetic activity of the leaves of *Tetracera indica* Merr.(Dilleniaceae) in vivo and in vitro, *J Med Plants Res* 6(49) (2012) 5912-22.
- [55] B. Chandrakar, A. Jain, S. Roy, V.R. Gutlapalli, S. Saraf, A. Suppahia, A. Verma, A. Tiwari, M. Yadav, A.J.J.O.P.R. Nayariseri, Molecular Modeling Of Acetyl-CoA Carboxylase (Acc) From *Jatropha Curcas* And Virtual Screening For Identification Of Inhibitors, *Journal of Pharmacy Research* 6(9) (2013) 913-918.
- [56] D. Ashok, M.G. Devulapally, V.K. Aamate, S. Gundu, S. Adam, S. Murthy, S. Balasubramanian, B. Naveen, T.J.J.O.M.S. Parthasarathy, Novel Pyrano [3, 2-B] Xanthen-7 (2h)-Ones: Synthesis, Antimicrobial, Antioxidant And Molecular Docking Studies, *Journal of Molecular structure* 1177 (2019) 215-228.
- [57] L.H. Abdel-Rahman, A.M. Abu-Dief, M.R. Shehata, F.M. Atlam, A.A.H.J.A.O.C. Abdel-Mawgoud, Some New Ag (I), Vo (Ii) And Pd (Ii) Chelates Incorporating Tridentate Imine Ligand: Design, Synthesis, Structure Elucidation, Density Functional Theory Calculations For Dna Interaction, Antimicrobial And Anticancer Activities And Molecular Docking Studies, *Applied Organometallic Chemistry* 33(4) (2019) E4699.
- [58] K. Díaz, L. Espinoza, R. Carvajal, M. Conde-González, V. Niebla, A.F. Olea, Y.J.I.J.O.M.S. Coll, Biological Activities And Molecular Docking Of Brassinosteroids 24-Norcholane Type Analogs, *International Journal of Molecular Sciences* 21(5) (2020) 1832.
- [59] S. Bouchagra, F. Benamia, Z.J.R.J.O.P.B. Djeghaba, C. Sciences, Docking Studies Of (-)-Epigallocatechin-3-Gallate: A Potential Non-Competitive Pancreatic Lipase Inhibitor., *Research Journal of Pharmaceutical, Biological and Chemical Sciences* 7(5) (2016) 2493-2505.
- [60] F.N. Ajeel, A.M. Khudhair, A. Mohammed, Research, Density functional theory investigation of the physical properties of dicyano pyridazine molecules, *International Journal of Science and Research* 4(4) (2015) 2334-2339.
- [61] T. Abbaz, A. Bendjeddou, D. Villemin, Density Functional Theory Studies On Molecular Structure And Electronic Properties Of sulfanilamide, Sulfathiazole, *IOSR Journal of Applied Chemistry* 12(1) (2019) 60-69.
- [62] B. Honarparvar, S.A. Pawar, C.N. Alves, J. Lameira, G.E. Maguire, J.R.A. Silva, T. Govender, H.G. Kruger, Pentacycloundecane lactam vs lactone norstatine type protease HIV inhibitors: binding energy calculations and DFT study, *Journal of biomedical science* 22(1) (2015) 15.
- [63] A. Bendjeddou, T. Abbaz, A. Gouasmia, D. Villemin, Molecular structure, HOMO-LUMO, MEP and Fukui function analysis of some TTF-donor substituted molecules using DFT (B3LYP) calculations, *International Research Journal of Pure and Applied Chemistry* 12(1) (2016) 1-9.
- [64] M. A.Iramain, A. E.Ledesma, S.A. Brandán, Structural properties and vibrational analysis of Potassium 5-Br-2-isonicotinoyltrifluoroborate salt. Effect of Br on the isonicotinoyl ring, *Journal of Molecular Structure* 1148 (2019) 146-156.

Journal Pre-proof

List of Figures

Fig. 1. General synthesis of anthraquinone precursor.

Fig. 2. General synthesis of pyrimidine precursor.

Fig. 3. Schematic synthesis of targeted anthraquinone based pyrimidine derivatives.

Fig. 4. Graphical representation of antioxidant activity and estimation of IC_{50} value by non-linear regression analysis in GraphPad Prism.

Fig. 5. Graphical representation of anti-diabetic activity and estimation of IC_{50} value by non-linear regression analysis in GraphPad Prism.

Fig. 6a. Leading pose of compound **G₁**, **G₂**, **G₃**, **G₄** into active pocket of 1HNY along with standard drug ACARBOSE; (**A1**) coupling of compound **G₁** with residues of 1HNY; (**A2**) coupling of compounds **G₂** with residues of 1HNY; (**A3**) coupling of compound **G₃** with residues of 1HNY; (**A4**) coupling of compound **G₄** with residues of 1HNY; (**A5**) coupling of compound **A5** (acarbose) with residues of 1HNY

Fig. 6b. 2D visualization of compound **G₁**, **G₂**, **G₃**, **G₄** by Discovery Studio Visualizer; (**A1**) 2D model of compound **G₁**; (**A2**) 2D model of compound **G₂**; (**A3**) 2D model of compound **G₃**; (**A4**) 2D model of compound **G₄**

Fig. 7a. Leading pose of compound **G₁**, **G₂**, **G₃**, **G₄** into active pocket of 3MN8 along with standard drug QUERCETIN: (**B1**) coupling of compound **G₁** with residues of 3MN8; (**B2**) coupling of compound **G₂** with residues of 3MN8; (**B3**) coupling of compound **G₃** with residues of 3MN8; (**B4**) coupling of compound **G₄** with residues of 3MN8; (**B5**) coupling of QUERCETIN with residues of 3MN8

Fig. 7b. 2D visualization of compound **G₁**, **G₂**, **G₃**, **G₄** by Discovery Studio Visualizer: (**B1**) 2D model of compound **G₁**; (**B2**) 2D model of compound **G₂**; (**B3**) 2D model of compound **G₃**; (**B4**) 2D model of compound **G₄**

Fig. 8. 2D schematic illustration by Discovery Studio Visualizer of reference compounds **A5** (Acarbose) and Quercetin

Fig. 9. The optimized geometry, numbering system, and the vector of the dipole moment of compound (G₁**-**G₄**) using B3LYP/3-21G(d).**

Fig. 10. Molecular Electrostatic Potential (MEP) of compounds (G₁**-**G₄**) based on DFT studies.**

Fig. 11. Frontier Molecular Orbitals of Compounds (G₁**-**G₄**).**

List of Figures

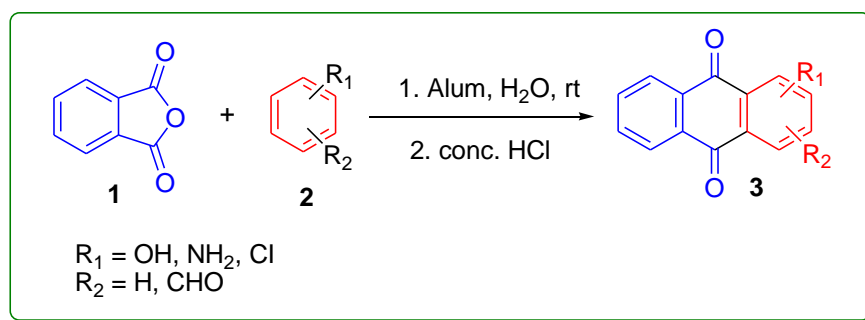


Fig. 1.

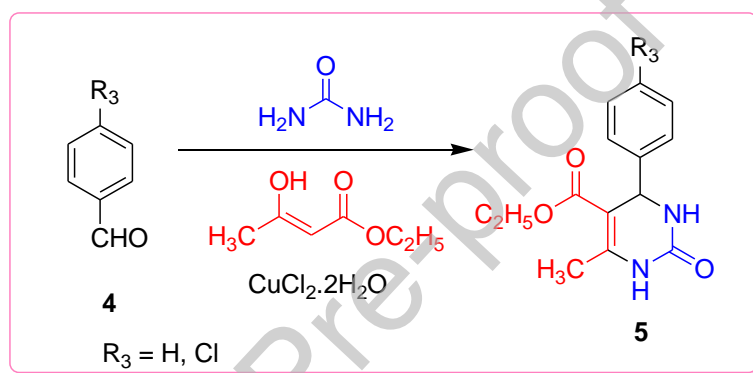


Fig. 2.

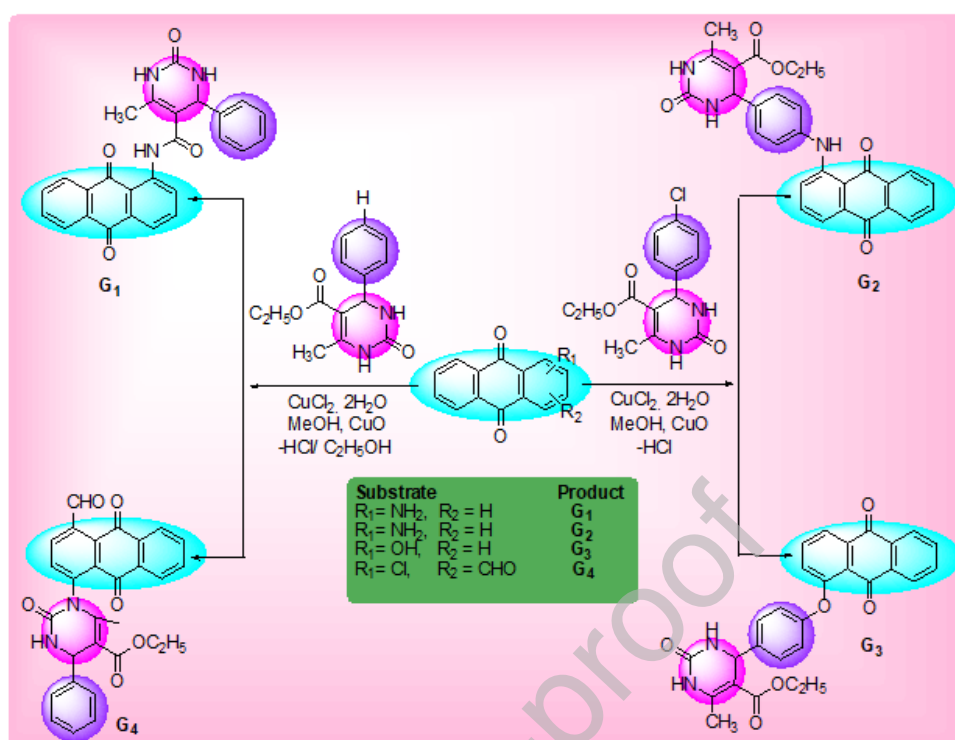


Fig. 3.

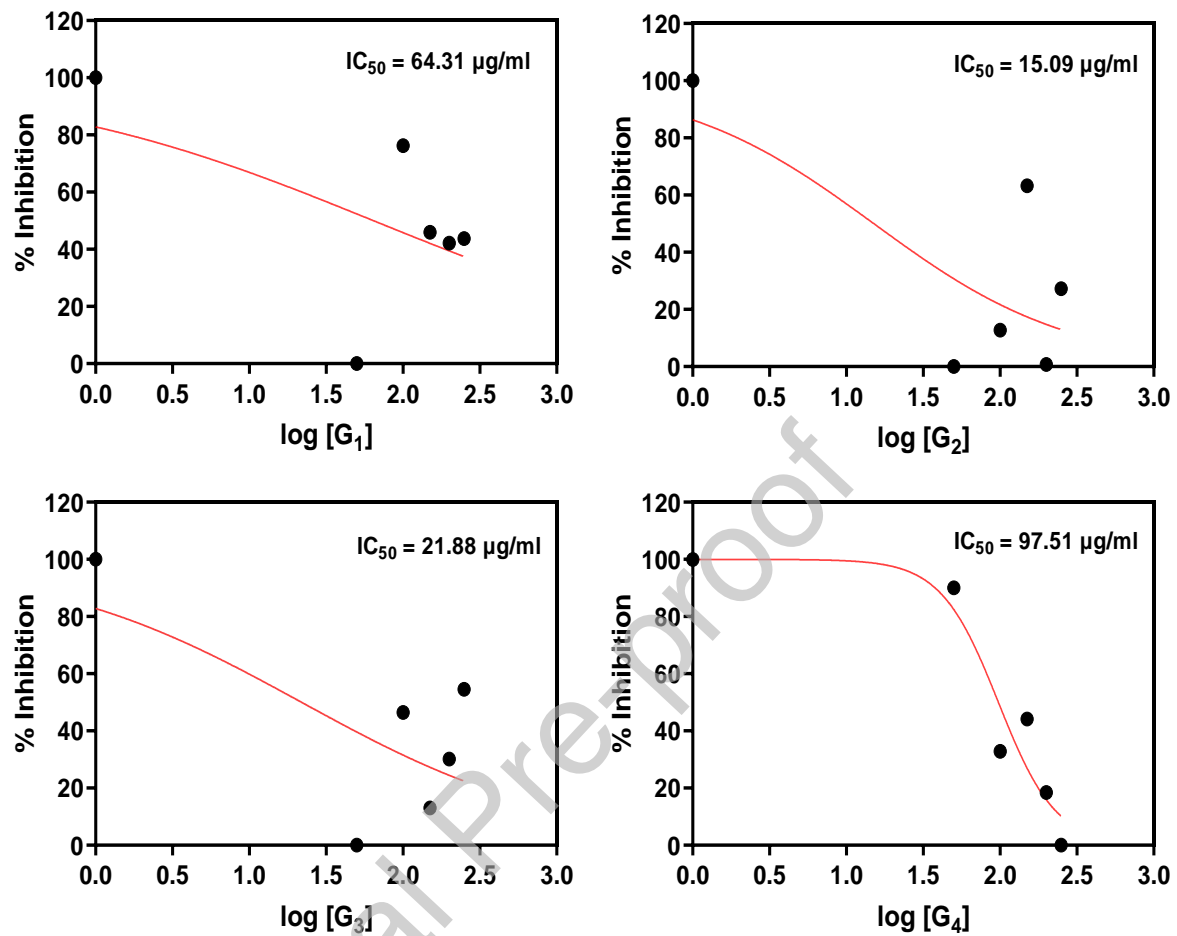


Fig. 4.

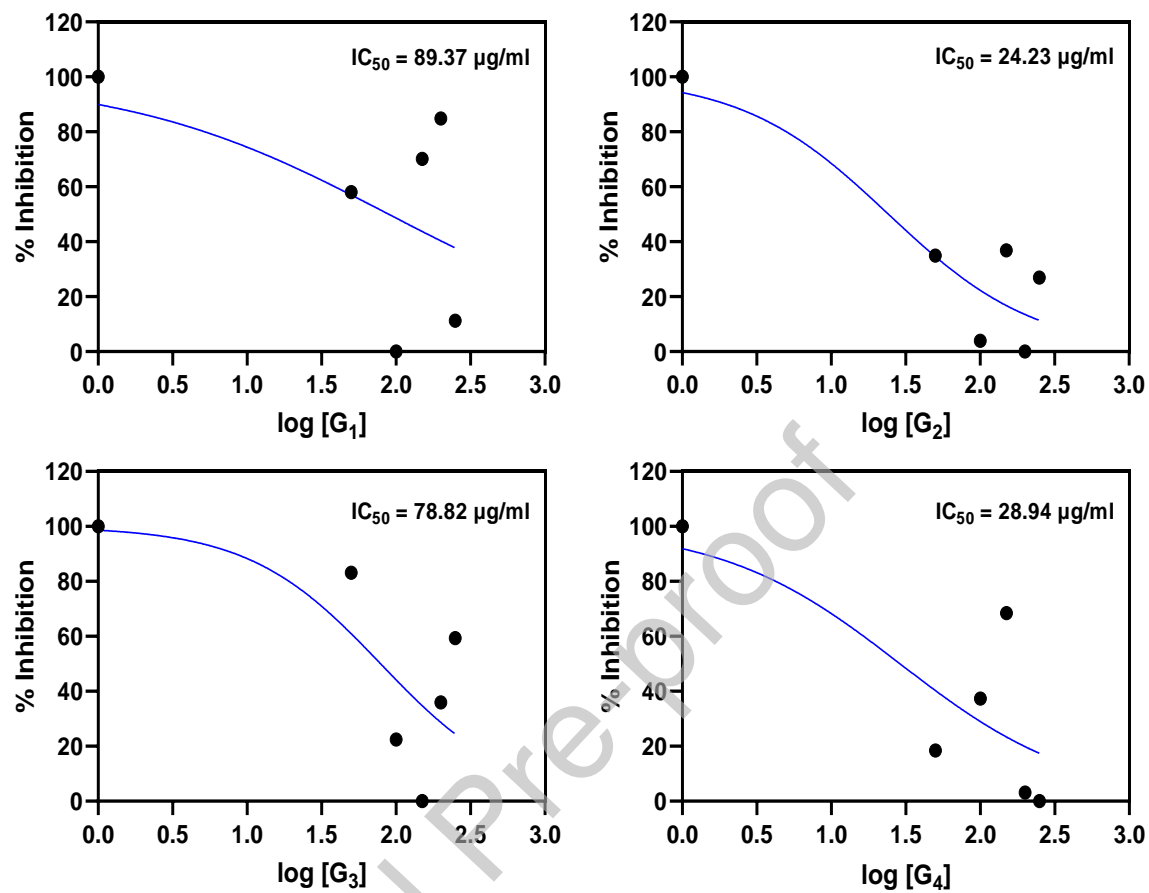


Fig. 5.

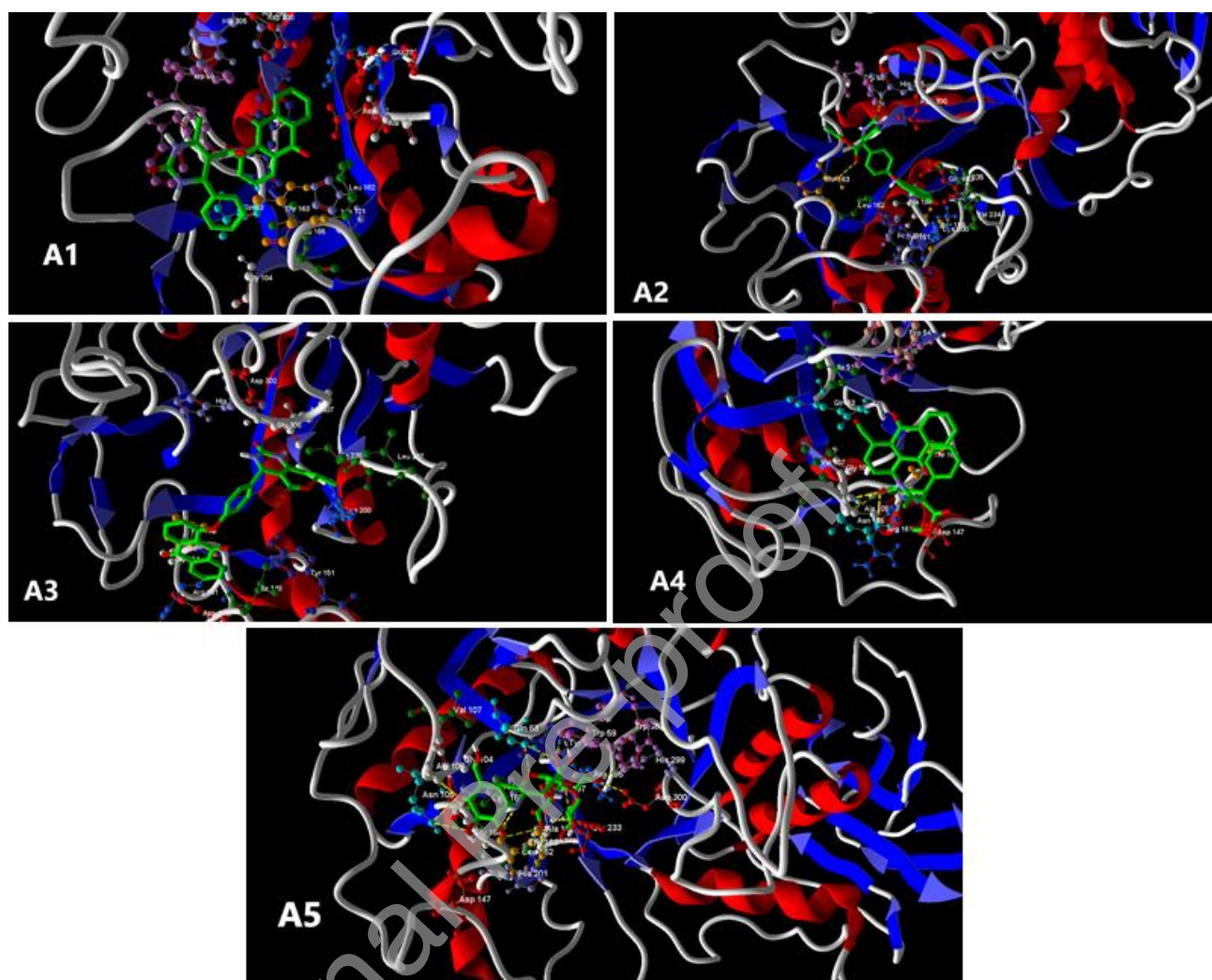


Fig. 6A

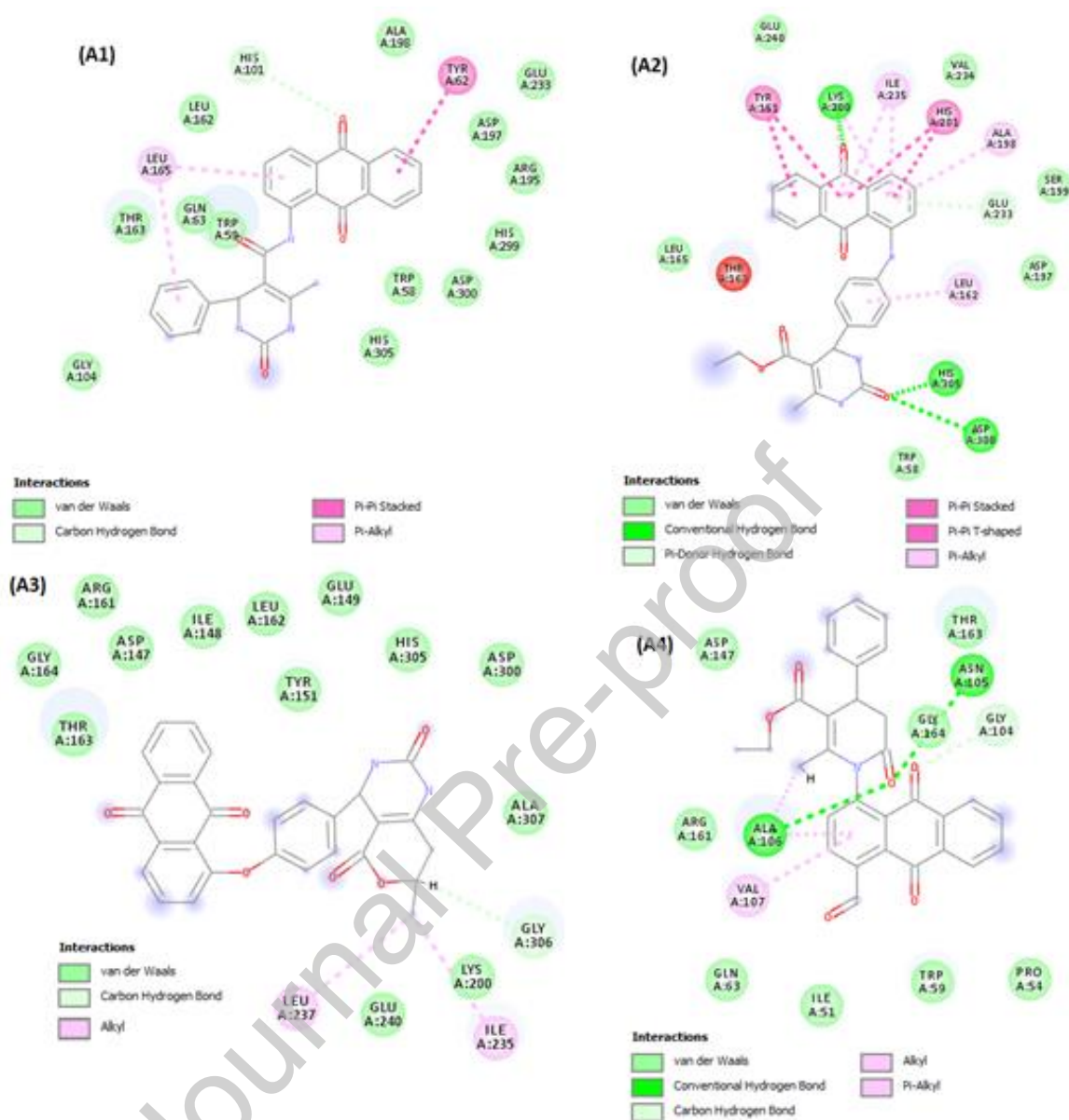


Fig. 6B

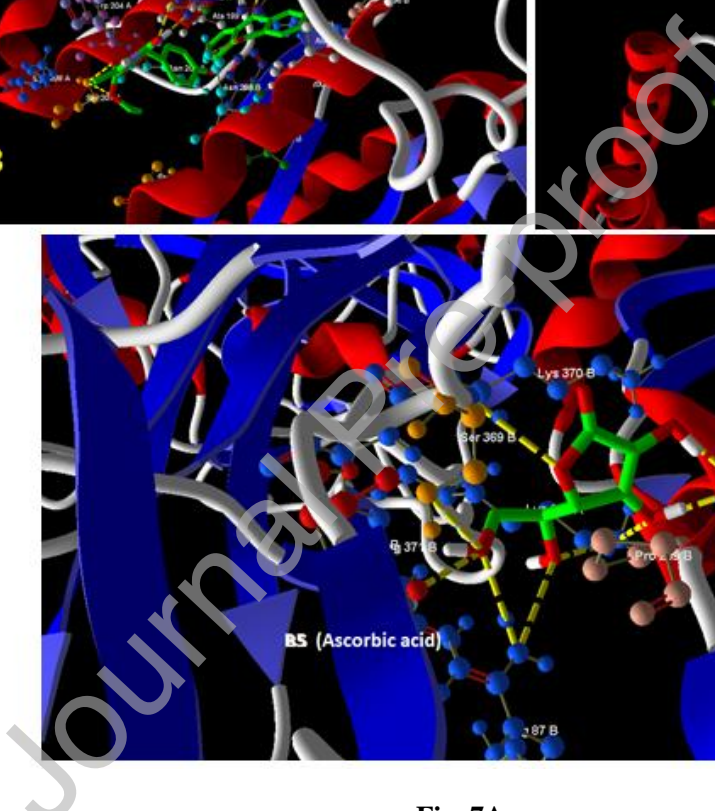


Fig. 7A

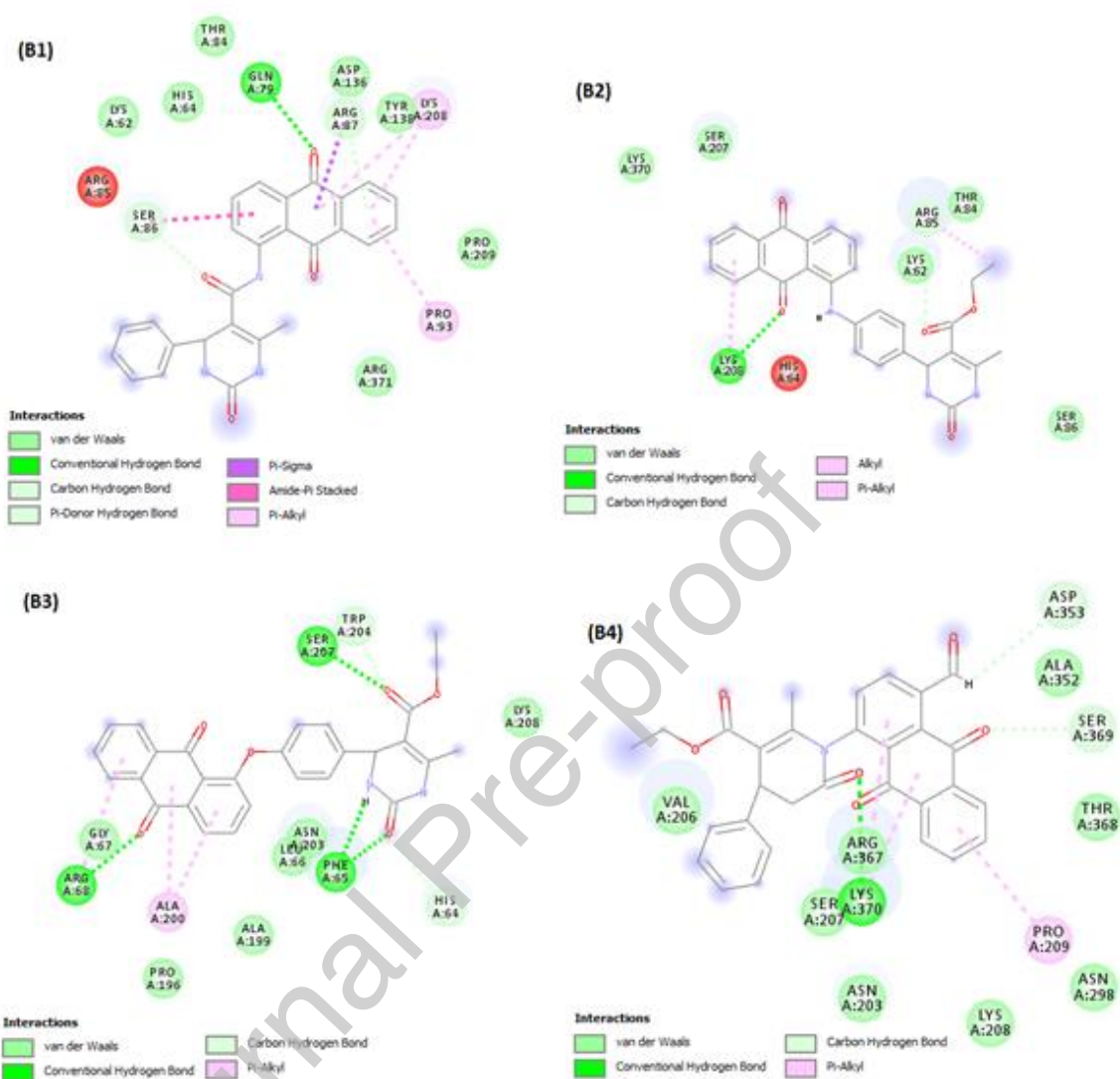


Fig. 7B

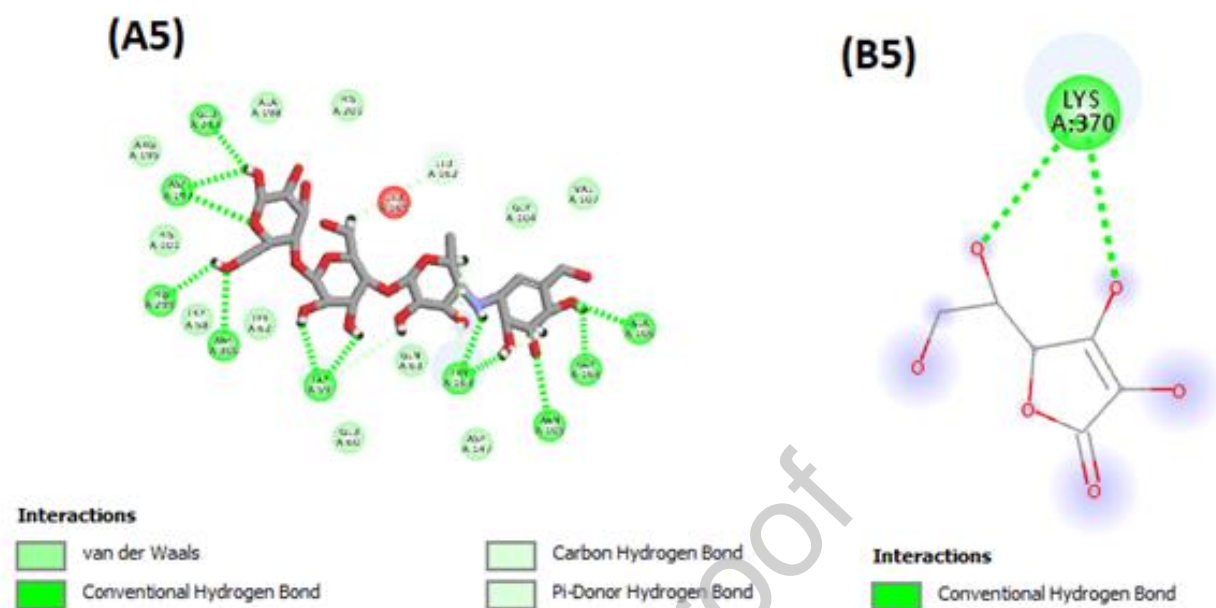


Fig. 8

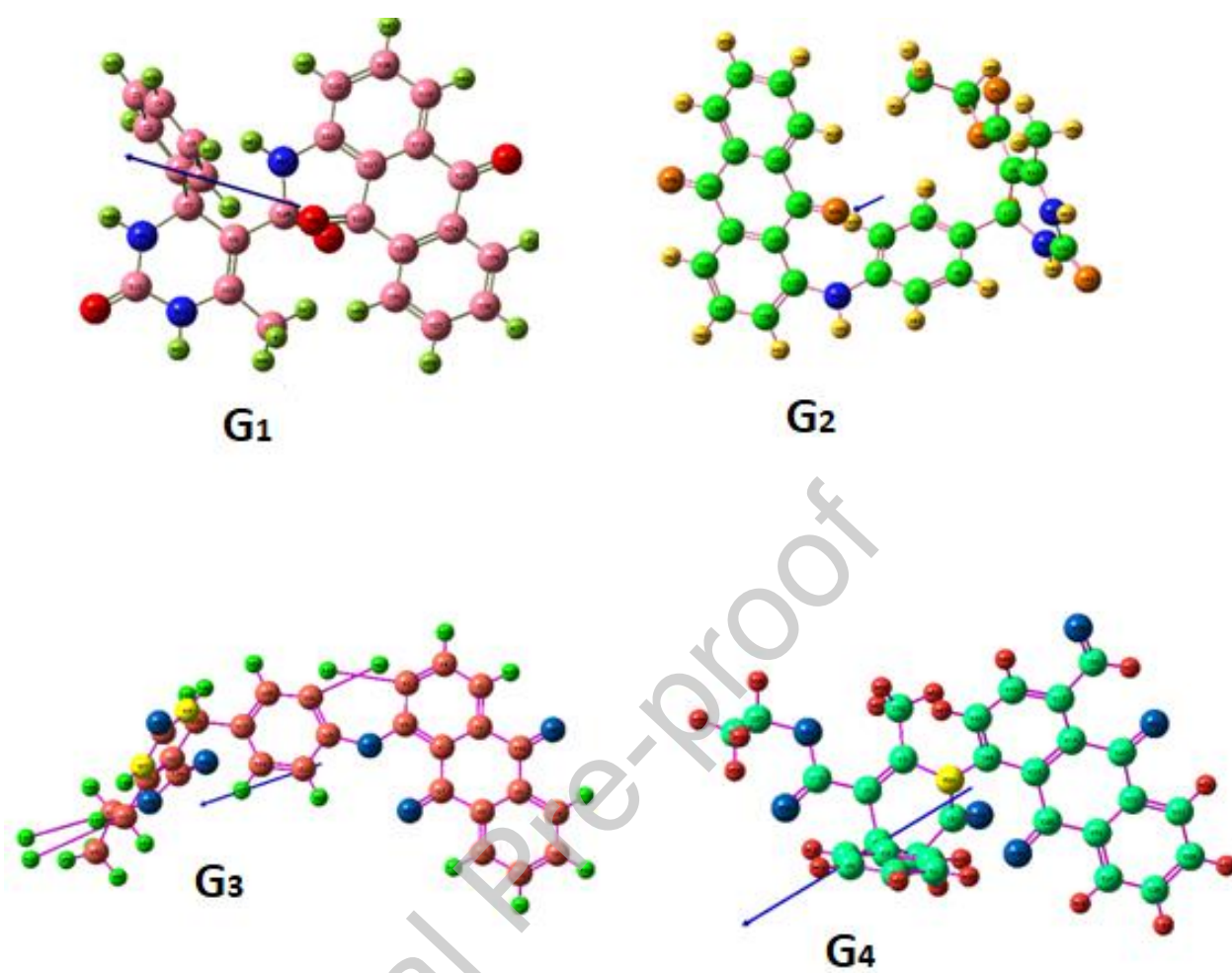


Fig. 9

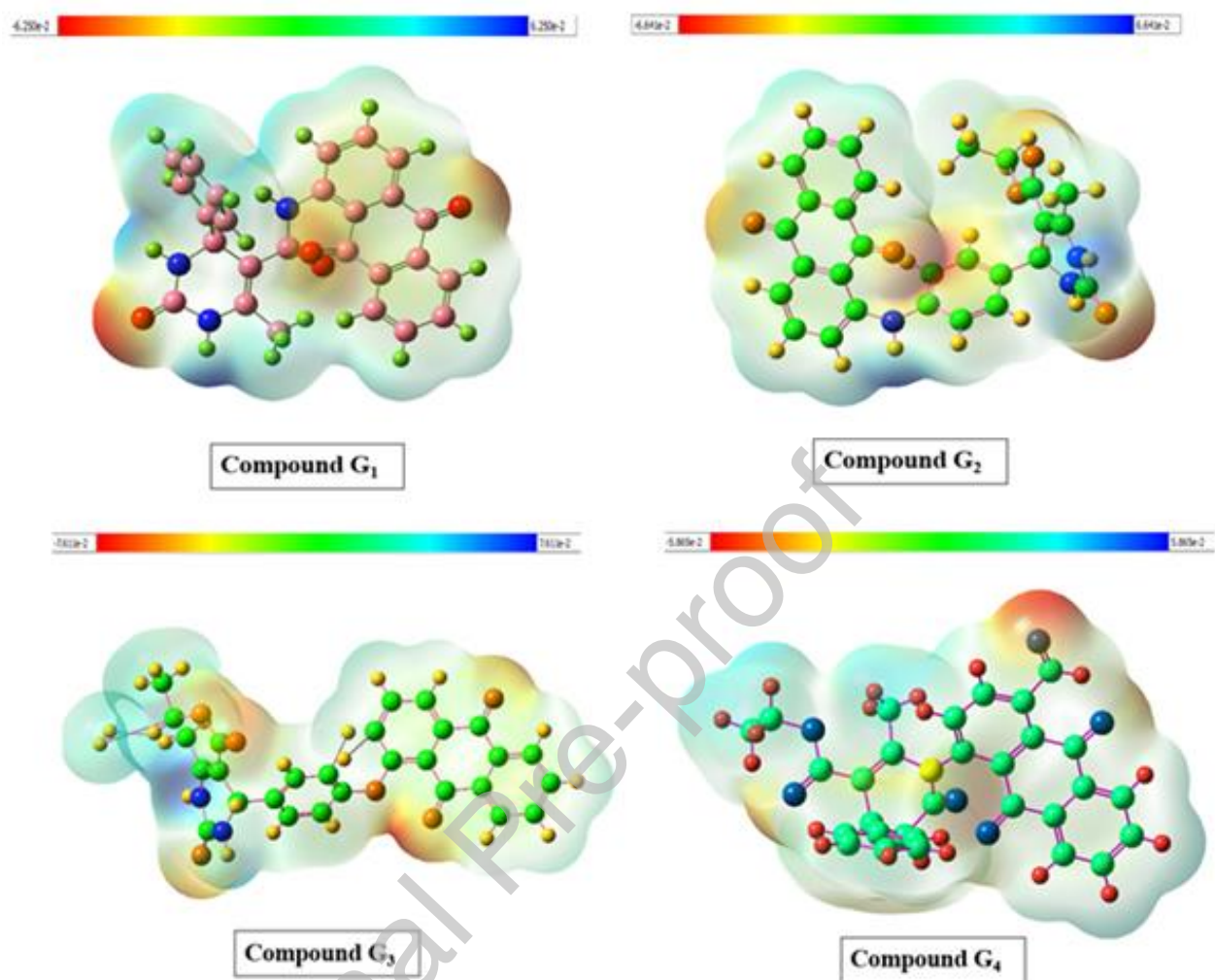


Fig. 10

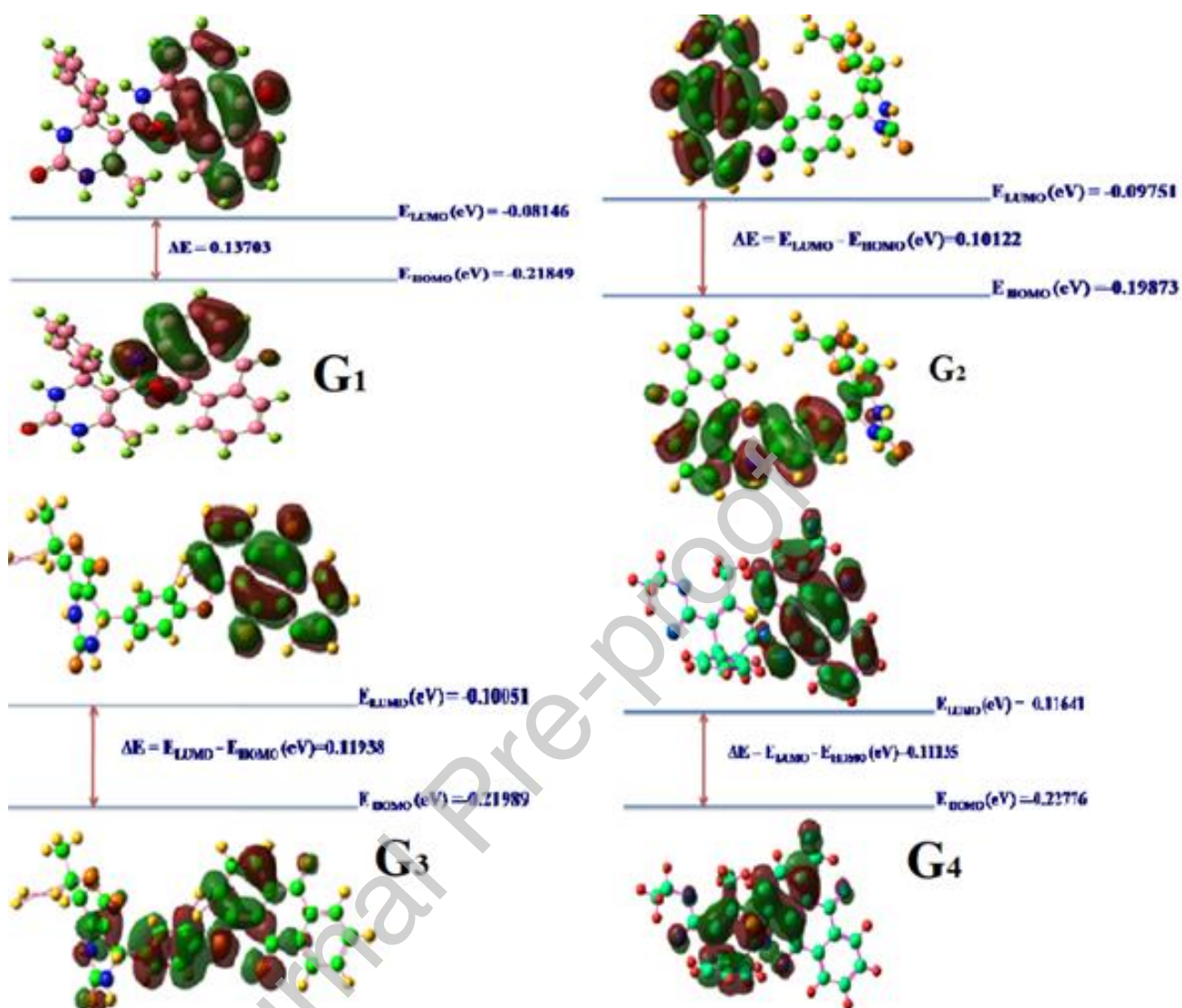


Fig. 11

List of Tables

Table 1. Percent inhibition of DPPH anti-oxidant activity of four compounds at varying concentration

Sr. No	Concentration ($\mu\text{g/ml}$)	Inhibition (%)			
		G ₁	G ₂	G ₃	G ₄
1	250	17.08	33.23	22.63	36.94
2	200	17.80	45.42	34.77	30.12
3	150	16.64	16.80	43.61	20.63
4	100	7.32	39.93	26.62	24.79
5	50	30.78	45.76	49.75	4.16

Table 2. Alpha amylase inhibitory effects of compounds G₁-G₄ at varying concentration

Sr. No	Concentration (µg/ml)	Inhibition (%)			
		G ₁	G ₂	G ₃	G ₄
1	250	36.35	42.20	15.43	39.36
2	200	6.21	57.80	24.29	38.12
3	150	12.23	36.52	37.94	12.41
4	100	40.96	55.50	29.43	24.65
5	50	17.20	37.59	6.38	32.09

Table 3. Molecular docking results of compounds G₁-G₄ docked into PDB:1NHY.

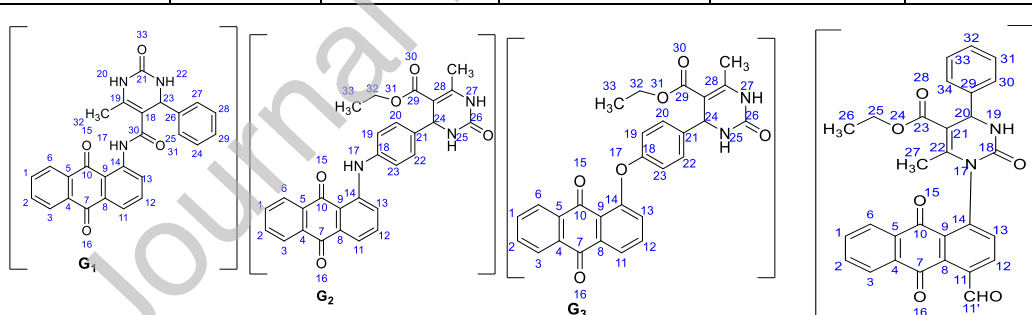
Sr. No	Compounds	Mol Dock Score (kcal/mol)	No. of Hydrogen Bonds	Groups in molecules interacting	Residues interacting	Hydrogen-bond length (in Å°)
	Acarbose	-111.57	09	15-OH 16OH 26-OH 28-OH 33-NH & 40-OH 42-OH 42-OH	Trp 59, Gln 63 Trp 59 Asp 197 His 299 Thr 163 Ala 106 Gly 164	2.93, 3.09 2.89 3.15 3.09 2.62 & 3.07 2.97 2.97
1	G ₁	-128.915	No interaction			
2	G ₂	-131.536	02	30-O O (26C=O)	Thr 163 His 305	2.602 2.44
3	G ₃	-123.501	No interaction			
4	G ₄	-119.481	01	O(11'-CHO)	Ile 235	2.89
						

Table 4. Molecular docking results of compounds G₁-G₄ docked into PDB: 3MN8.

Sr. No	Compounds	Mol Dock Score (kcal/mol)	No. of hydrogen bonds	Groups in molecules interacting	Residues interacting	Hydrogen-bond length (in Å)
	Ascorbic acid	-80.346	08	8-O 9-OH & 10-OH 10-OH & 11-OH 11-OH & 12-OH 12-OH	Lys 370 Ser 207 Lys 370 Arg 87 Ser 369	3.28 2.83 & 2.95 3.09 & 3.14 3.14 & 3.10 3.16
1	G ₁	-133.291	03	15-O 16-O 31-O	Lys 370 Gln 79 Ser 86	2.72 2.61 3.27
2	G ₂	-184.273	02	15-O O(26-CO)	Lys 208 Arg 367	3.091 3.093
3	G ₃	-150.528	06	15-O 25-NH & O (26C=O) 16-O 30-O & 31-O	Arg 68 Phe 65 Asn 203 Ser 207	3.58 2.60, 3.31 3.41 3.10, 2.60
4	G ₄	-131.96	03	O(11-CHO) 15-O & 28-O	Lys 370 Asn 203	3.108 3.17, 3.01

Note: structural formulas and numberings are same as for above.

Table 5. Quantum chemical parameters based upon DFT computations for the purpose of SAR studies at DFT/B3LYP/3-21G.

Parameters	Structure Activity Relationship			
	G ₁	G ₂	G ₃	G ₄
E _{HOMO} (eV)	-0.21849	-0.19873	-0.21989	-0.22776
E _{LUMO} (eV)	-0.08146	-0.09751	-0.10051	-0.11641
Energy Gap “ $\Delta E = E_{LUMO} - E_{HOMO}$ (eV)”	0.13703	0.10122	0.11938	0.11135
Dipole Moment “ μ (Debye)”	2.141	0.9706	5.470	3.176
Chemical Hardness “ η (eV)”	0.068515	0.05061	0.05969	0.055675
Chemical Softness “S”	7.297	9.8794	8.3766	8.980
Electro negativity “ χ (eV)”	0.1499	0.14812	0.1602	0.1720
Electrophilicity Index “ ω ”	0.07495	0.07406	0.0801	0.086
Ionization Potential “I = - E _{HOMO} (eV)”	0.21849	0.19873	0.21989	0.22776
Electronic Energy “E (Hartree)”	-1459.28	-1612.35	-1632.07	-1654.00
Chemical Potential “CP”	-0.1499	-0.14812	-0.1602	-0.1720
Nucleophilicity Index “N”	13.342	13.50	12.484	11.627

Graphical Abstract

